

# Time-domain based feature space at FLUXNET sites for vegetation patterns identification

Daniela Vanella

Dipartimento di Agricoltura,  
Alimentazione e Ambiente (Di3A)  
University of Catania  
Catania, Italy  
daniela.vanella@unict.it

Juan Miguel Ramírez-Cuesta

Dpto. Riego  
Centro de Edafología y Biología  
Aplicada del Segura (CEBAS-CSIS)  
Murcia, Spain  
ramirezcuesta.jm@gmail.com

Simona Consoli

Dipartimento di Agricoltura,  
Alimentazione e Ambiente (Di3A)  
University of Catania  
Catania, Italy  
simona.consoli@unict.it

Antonio Motisi

Dipartimento di Scienze Agrarie,  
Alimentari e Forestali (SAAF)  
University of Palermo  
Palermo, Italy  
antonio.motisi@unipa.it

Mario Minacapilli

Dipartimento di Scienze Agrarie,  
Alimentari e Forestali (SAAF)  
University of Palermo  
Palermo, Italy  
mario.minacapilli@unipa.it

**Abstract**—Monitoring the flux transfer of mass and energy occurring within the soil-plant-atmosphere continuum is a pivotal key for understanding hydrological and vegetation relationships. Average daily values of the Priestley - Taylor (PT) parameter were calculated for 4 eddy covariance (EC) flux tower sites from FLUXNET network, characterized by different vegetation features, over the 2010-12 reference period. Site-by-site feature spaces (built by difference in diurnal and night-time land surface temperature versus enhanced vegetation index,  $\Delta LST-EVI$ ) were obtained by combining satellite data (MODIS) and observed PT parameter ( $\phi$ ) retrieved by FLUXNET surface energy balance (SEB) fluxes. The results revealed the capability of satellite time-series data to monitor seasonal changes in  $\phi$ . This preliminary observation offers a promising tool for exploring the feature spaces in respect to the time, helping to retrieve useful information for environmental monitoring.

**Keywords**—Eddy covariance, EVI, Land Surface Temperature, surface energy balance fluxes

## I. INTRODUCTION

Evapotranspiration (ET) is one of the fundamental processes controlling the equilibrium within the soil-plant-atmosphere continuum. In this view, micrometeorological monitoring (e.g. FLUXNET) offers robust surface energy balance (SEB) fluxes observations. Each site of the global FLUXNET network is equipped with eddy covariance (EC) towers for measuring the exchanges of mass and energy between terrestrial ecosystems and the atmosphere (<https://fluxnet.ornl.gov/>). At the field level, FLUXNET network is mainly used for the validation of ET estimates obtained at larger scale by remote sensing (RS)-based applications. Within the numerous RS-based models used for determining ET [1], the Priestley-Taylor (PT) method [2] has been implemented in various environmental scenarios [3]. The PT method uses the feature space of land surface temperature (LST) and vegetation indices (VIs) for modelling the PT parameter ( $\phi$ ). A number of studies improved the original concept based on LST-VI feature space proposed by [4] adopting different VIs, as normalized difference vegetation index - NDVI, enhanced vegetation index - EVI and fraction cover -  $F_c$  (e.g. [5]). Other authors adopted the difference between diurnal and night-time LST ( $\Delta LST$ ), instead of the LST, for improving the accuracy of explaining the resistance of the surface to external temperature variations [6].

A step-forward in LST-VI feature space consisted in the exploration of LST and VI time-series [7, 8]. From a qualitative point-of-view, the feature spaces obtained considering the time domain contribute to observe environmental phenomena in time as  $\phi$  changes. The aim of this study was to combine EC data with  $\Delta LST$  and EVI time-series to assess the vegetation patterns of two forest types (evergreen needleleaf and deciduous broadleaved) in 4 FLUXNET sites (ITRen, ITLav, ITCol, ITRo2). This research represents a preliminary step towards for determining if satellite time-series data can be used as a tool to monitor the seasonal changes in  $\phi$  and to classify forest types.

## II. MATERIALS AND METHODS

### A. The Priestley-Taylor model and LST-VI feature space

The PT model is based on the concept of equilibrium evaporation postulated by [9]. Equilibrium evaporation conditions rarely exist in natural environments, due to variations of surface and/or atmospheric conditions (e.g., [10]). To compensate these deviations, [2] adjusted the equilibrium evaporation model via an empirical parameter ( $\phi$ ), which relates actual evaporation to equilibrium evaporation. The PT model for estimating latent heat flux (LE) is:

$$LE = \phi \cdot (R_n - G) \cdot \frac{s}{s + \gamma} \quad (1)$$

where,  $R_n$  is surface net radiation ( $W m^{-2}$ ),  $G$  is the soil heat flux ( $W m^{-2}$ );  $S$  is the slope of the saturated vapour pressure versus air temperature ( $kPa K^{-1}$ ) calculated as reported in [11]; and  $\gamma$  is the psychrometric constant ( $kPa K^{-1}$ ) computed using the atmospheric pressure derived as function of the elevation (m. a.s.l.) of the region of interest.

Values of  $\phi$  have been shown to be generally constant (e.g., 1.26) in environment where surface is fully covered by vegetation without evaporation restriction (REF). However, authors showed that  $\phi$  varied over time and space in different ecosystems, observing large deviations in  $\phi$  under drier or varied vegetation conditions [12]. The LST-VI feature space (or triangle method) allowed modelling  $\phi$  using interpolation schemes from the two boundary conditions of the LST-VI feature space (i.e. warm and cold edge). According to [7], the parameterization of the two boundary conditions of the feature space can be performed for each single pixel by

exploring the temporal variability of LST–VIs obtained by satellite time series.

### B. FLUXNET sites

FLUXNET data were used for calculating  $\phi$  at the selected demo-sites within the reference period 2010-12 (except for ITRen and ITRo2, where EC data were available only for 2010-11) by rearranging (1), as follows:

$$\phi = \frac{LE}{(R_n - G) \cdot \frac{s}{s+y}} \quad (2)$$

The EC demo-sites used in this study referred to 2 different land uses (Tab.1), with EC measurement height varied from 32 m at ITCol [13] to more than 40 m in ITLav and ITRen [14]. Table 1 and Table 2 report the main demo-sites characteristics and the details on the measurements period (in terms of DOY, day-of-the-year) considered in this study, respectively.

Semi-hourly EC data (net radiation,  $R_n$ ; soil heat flux,  $G$ ; latent heat flux,  $LE$ , and sensible heat flux,  $H$ ) and air temperature ( $T_{air}$ ) data were averaged at the MODIS temporal step (8-day).

TABLE I. FLUXNET DEMO-SITES CHARACTERISTICS

FLUXNET demo-site	Lat. (dd)	Long. (dd)	Elev. (m)	$T_{air}$ (°C)	EC height (m)
<i>ITRen</i>	46.59	11.43	1730	4.7	40
<i>ITLav</i>	45.96	11.28	1353	7.8	33
<i>ITCol</i>	41.85	13.59	1560	6.3	32
<i>ITRo2</i>	42.39	11.92	160	15.2	-

TABLE II. FLUXNET MEASUREMENTS PERIOD

FLUXNET demo-site	DOYs	Years
<i>ITRen</i>	193-361	2010-2011
<i>ITLav</i>	193-361	2010-2012
<i>ITCol</i>	193-361	2010-2012
<i>ITRo2</i>	193-361	2010-2011

### C. Satellite products

MODIS time series of LST (MOD11A2) and EVI (MOD13A1). were extracted at each EC demo-sites. LST and EVI data (provided respectively by Terra and Terra/Aqua sensors) were obtained from the Land Processes Distributed Active Archive Centre (LP DAAC <http://lpdaac.usgs.gov/>). Specifically, MOD11A2 (with 1000 m of spatial resolution) provides an average 8-day per-pixel LST. Both daytime and night-time products from MOD11A2 were combined for calculating the difference of diurnal and night-time LST ( $\Delta LST$ ). The algorithm for EVI product (MOD13A1, with 500 m of spatial resolution), offered the best available pixel value from all the acquisitions from the 16 day period, as function of low clouds, low view angle, and the highest NDVI/EVI value. The EVI 8-day phasing, included in the production of the 16-day composites between Terra and Aqua sensors, allowed the generation of a combined 8-day EVI time series. The number of selected MODIS/Terra and Terra/Aqua overpasses was of 104, between DOY 193 2010 and DOY 321 2012.

## III. RESULTS AND DISCUSSION

The summary of the main statistics values (averages and standard deviation) of SEB fluxes ( $LE$ ,  $R_n$ ,  $G$ ,  $H$ ),  $T_{air}$  and  $\phi$  obtained at the EC demo-sites are reported in Table 3 (please refer to Table 2 for measurements period).

As expected, the evergreen demo-sites (ITRen and ITLav) showed higher average daily  $LE$  rates than the deciduous sites (ITCol and ITRo2), with average values of  $79.79 \text{ W m}^{-2}$  versus  $59.29 \text{ W m}^{-2}$ , respectively for forest types (Tab.2). Also  $\phi$  showed the same trend, with values of  $0.66$  versus  $0.59$  at the evergreen and deciduous forest sites, respectively. As reported in Tab.1, the evergreen demo-sites (ITRen and ITLav), characterized by analogous climate condition in terms of similar latitude/altitude conditions, showed average daily  $R_n$  and  $T_{air}$  values of  $252.10 \text{ W m}^{-2}$  and  $7.49 \text{ °C}$ , respectively (Tab.3). Conversely, the different latitude/altitude conditions occurred at the deciduous sites (ITCol and ITRo2, Tab.3) influenced the range of variability of the average daily  $R_n$  and  $T_{air}$  fluxes, showing values of  $241.77 \text{ W m}^{-2}$  and  $11.71 \text{ °C}$ , respectively (Tab.3). The same behaviour was observed for  $G$  and  $H$  fluxes (Tab.3).

TABLE III. AVERAGES EC FLUXES ( $R_n$ ,  $G$ ,  $LE$  AND  $H$ ) AND PARAMETERS ( $T_{air}$  AND  $\phi$ ) MEASURED AT THE EC DEMO-SITES

FLUXNET demo-site	$LE$ $\text{W m}^{-2}$	$R_n$ $\text{W m}^{-2}$	$G$ $\text{W m}^{-2}$	$H$ $\text{W m}^{-2}$	$T_{air}$ $\text{°C}$	$\phi$ [-]
<i>ITRen</i>	92.47 ( $\pm 69.70$ )	244.41 ( $\pm 118.10$ )	0.36 ( $\pm 3.33$ )	152.14 ( $\pm 71.88$ )	6.53 ( $\pm 6.80$ )	0.79 ( $\pm 0.45$ )
<i>ITLav</i>	65.32 ( $\pm 46.34$ )	259.78 ( $\pm 107.73$ )	-0.75 ( $\pm 5.58$ )	105.85 ( $\pm 60.84$ )	8.46 ( $\pm 6.94$ )	0.53 ( $\pm 0.29$ )
<i>ITCol</i>	60.15 ( $\pm 56.94$ )	290.77 ( $\pm 123.16$ )	-0.27 ( $\pm 2.16$ )	100.94 ( $\pm 56.94$ )	10.16 ( $\pm 7.82$ )	0.34 ( $\pm 0.19$ )
<i>ITRo2</i>	58.43 ( $\pm 60.53$ )	192.78 ( $\pm 112.77$ )	-4.74 ( $\pm 11.48$ )	48.96 ( $\pm 37.88$ )	13.26 ( $\pm 8.21$ )	0.83 ( $\pm 0.46$ )

Figs 1-4 showed the  $\Delta LST$ -EVI feature spaces obtained at the EC demo-sites. A close dependence of the feature spaces to the measured  $\phi$  changes were observed at the different sites.

In general, the shape of the feature spaces varied as function of the land uses. A globular pattern was observed for the evergreen forests (ITRen and ITLav, Figs 1-2 a,b); whereas a double globular pattern was recognized at the two deciduous forest sites (ITCol and ITRo2, Figs 3-4 a,b). These different shapes reproduce the phenological stages of the leaves activity/inactivity at the 2 forest types. Additionally, the altitude/latitude effect was also appreciated in the feature-spaces distribution. Thus, ITRen and ITLav (in Figs.1-2 a,b) showed similar feature space distributions because they referred to the same latitude (altitude) (Tab. 1). Conversely, despite being both deciduous broadleaf forests, a different feature space pattern was observed between ITCol and ITRo2 (Figs. 3-4 a,b), those referred to different latitude (altitude) (Tab.1).

According to [15], at the evergreen needleleaf forest sites (ITRen and ITLav), characterized by high biomass, the seasonal variations in  $\phi$  ( $0.66 \pm 0.18$ ) were poor evident, due to EVI values stability within the range  $0.2$ - $0.5$  and  $\Delta LST$  values within the range  $0$ - $15 \text{ °C}$  (Figs. 1-2a).

The  $\Delta LST$ -EVI patterns were coherent with the expected strong seasonal dynamics of EVI (range of  $0.2$ - $0.7$ ) and  $\Delta LST$

(range of 0–23 °C) occurring at the deciduous broadleaf forests (ITCol and ITRo2, Figs. 3–4b). For these sites, the  $\phi$  derived by EC fluxes collected during Winter – Autumn (DOYs 0–100 and 250–360), corresponded to smaller EVI values and as well as slighter  $\Delta LST$  values in respect to the Spring–Summer interval, characterized by higher EVI and  $\Delta LST$  values. This is more evident at ITRo2, where the  $\Delta LST$  values were greater than ITCol, due to the wide variability of LST between day and night (up to 23 °C) and  $\phi$  (ranged between -0.39 and 2.30).

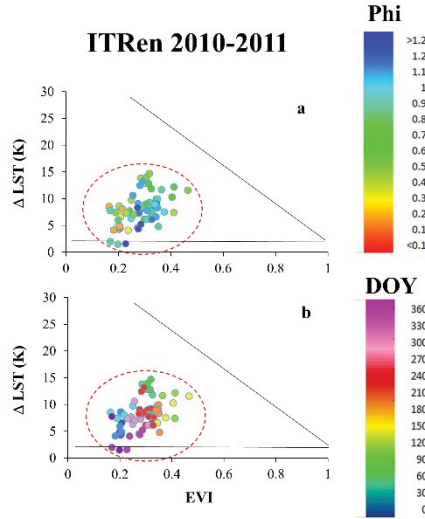


Fig. 1. Time-domain based feature spaces obtained for ITRen (evergreen needleleaf forest) during the period of fluxes measurements (2010–2011): dependance of  $\Delta LST$ -EVI values with the measured Priestley–Taylor  $\phi$  parameter (a) and DOY (b).

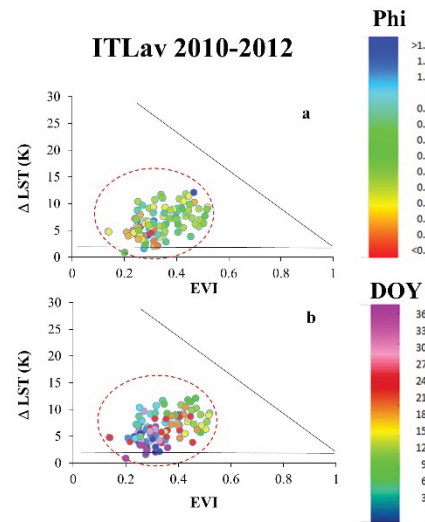


Fig. 2. Time-domain based feature spaces obtained for ITLav (evergreen needleleaf forest) during the period of fluxes measurements (2010–2012): dependance of  $\Delta LST$ -EVI values with the measured Priestley–Taylor  $\phi$  parameter (a) and DOY (b).

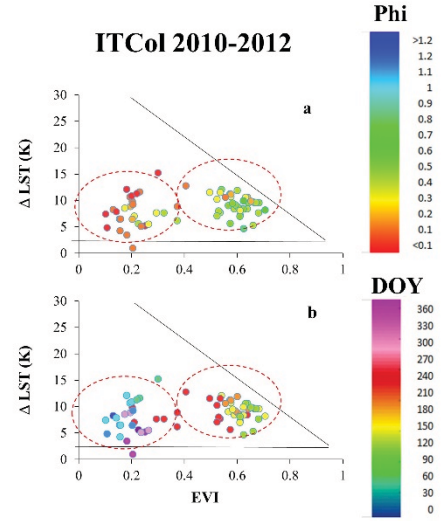


Fig. 3. Time-domain based feature spaces obtained for ITCol (deciduous broadleaf forest) during the period of fluxes measurements (2010–2012): dependance of  $\Delta LST$ -EVI values with the measured Priestley–Taylor  $\phi$  parameter (a) and DOY (b).

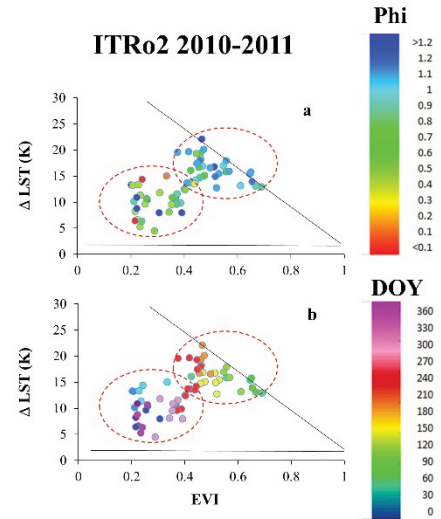


Fig. 4. Time-domain based feature spaces obtained for ITRo2 (deciduous broadleaf forest) during the period of fluxes measurements (2010–2011): dependance of  $\Delta LST$ -EVI values with the measured Priestley–Taylor  $\phi$  parameter (a) and DOY (b).

#### IV. CONCLUSION

Average daily values of  $\phi$  were calculated for 4 EC flux tower sites with contrasting vegetation and altitude/latitude characteristics on Italy over the 2010–12 reference period. The results revealed the capability of satellite time-series data for monitoring seasonal changes in  $\phi$ . This preliminary observation offers a promising tool for exploring the feature spaces in respect to the time, helping to retrieve useful feature for environmental monitoring. Moreover, these results highlight the seasonal behaviour of land surfaces in terms of  $\phi$  changes, providing useful insights for land uses classification with remote-sensing data.

## ACKNOWLEDGMENT

The authors thank the EU, the Italian Ministry of Education, Universities and Research and the Spanish Agencia Estatal de Investigación for funding, as part of the collaborative international consortium IRIDA (“Innovative remote and ground sensors, data and tools into a decision support system for agriculture water management”), financed under the ERA-NET Cofund WaterWorks 2014. This ERA-NET is an integral part of the 2015 Joint Activities developed by the Water Challenges for a Changing World Joint Programme Initiative (Water JPI).

## REFERENCES

- [1] S. Consoli, D. Vanella (2014). Comparisons of satellite-based models for estimating evapotranspiration fluxes. *Journal of Hydrology* 513, 475–489;
- [2] C.H.B. Priestley, R.J. Taylor (1972). On the Assessment of Surface Heat Flux and Evaporation Using Large-Scale Parameters. *Monthly Weather Review* 100(2):81-92.
- [3] Y. Yao, S. Liang, X. Li, J. Chen, K. Wang, K. Jia, J. Chen, B. Jiang, J.B. Fischer, Q. Mu, T. Grünwald, C. Bernhofer, O. Roupsard (2015). A satellite-based hybrid algorithm to determine the Priestley–Taylor parameter for global terrestrial latent heat flux estimation across multiple biomes. *Remote Sensing of Environment*, 165, 216-233.
- [4] L. Jiang, S. Islam, (1999). A methodology for estimation of surface evapotranspiration over large areas using remote sensing observations. *Geophysical Research Letters*, 26, 2773–2776.
- [5] X. Yang, J.J. Wu, P.J. Shi, F. Yan (2008). Modified triangle method to estimate soil moisture status with MODerate resolution Imaging Spectroradiometer (MODIS) products. *Proc. Int. Arch. Photogramm. Remote Sens. Spat. Inf. Sci.*, 37, 555-560.
- [6] W.P. Kustas, J.M. Norman, M.C. Anderson, A.N. French. (2003). Estimating subpixel surface temperatures and energy fluxes from the vegetation index–radiometric temperature relationship. *Remote Sensing of Environment*, 85, 429–440.
- [7] M. Minacapilli, S. Consoli, D. Vanella, G. Ciraolo, A. Motisi (2016). A time domain triangle method approach to estimate actual evapotranspiration: application in a Mediterranean region using MODIS and MSG-SEVIRI products. *Remote Sensing of Environment* 174, 10-26
- [8] S. Stisen, I. Sandholt, A. Nørgaard, R. Fensholt, K.H. Jensen (2008). Combining the triangle method with thermal inertia to estimate regional evapotranspiration—Applied to MSG-SEVIRI data in the Senegal River basin. *Remote Sensing of Environment*, 112(3), 1242–1255.
- [9] R.O. Slatyer, I.C. McIlroy, (1967). *Practical Microclimatology*. CSIRO, Melbourne, Australia.
- [10] W.E. Eichinger, M.B. Parlange, H. Stricker (1996). On the Concept of Equilibrium Evaporation and the Value of the Priestley-Taylor Coefficient. *Water Resources Research* 32:161-164.
- [11] R.G. Allen, L. Pereira, D. Raes, M. Smith (1998) *Crop evapotranspiration-Guidelines for computing crop water requirements-FAO Irrigation and drainage paper 56*. FAO, Rome, 300, 6541.
- [12] Y. Yao, S. Liang, J. Yu, S. Zhao, Y. Lin, K. Jia, X. Zhang, J. Cheng, X. Xie, L. Sun, X. Wang, L. Zhang (2017). Differences in estimating terrestrial water flux from three satellite-based Priestley-Taylor algorithms. *International journal of applied earth observation and geoinformation*, 56, 1-12.
- [13] P.C. Stoy et al. (2013). A data-driven analysis of energy balance closure across FLUXNET research sites: The role of landscape scale heterogeneity. *Agricultural and Forest Meteorology* 171: 137-152.
- [14] A. Cescatti, B. Marcolla (2004). Drag coefficient and turbulence intensity in conifer canopies. *Agricultural and forest meteorology*, 121(3), 197-206.
- [15] M. Yebra, A. Van Dijk, R. Leuning, A. Huete, J.P. Guerschman (2013). Evaluation of optical remote sensing to estimate actual evapotranspiration and canopy conductance. *Remote Sensing of Environment*, 129, 250-261.